Greenhouse Gas Footprint, Water-Intensity, and, Production Cost of Bio-Based Isopentenol as a Renewable Transportation Fuel

Nawa Raj Baral [a,b], Olga Kavvada [a,c], Daniel Mendez Perez[a,b], Aindrila Mukhopadhyay[a,b], Taek Soon Lee[a,b], Blake A. Simmons[a,b], Corinne D. Scown*[a,b,c]

[a]Joint BioEnergy Institute, Lawrence Berkeley National Laboratory, 5885 Hollis Street, Emeryville, California 94608, United States

[b]Biological Systems and Engineering Division, Lawrence Berkeley National Laboratory, 1 Cyclotron Road, Berkeley, California 94720, United States

[c]Energy Analysis and Environmental Impacts Division, Lawrence Berkeley National Laboratory, 1 Cyclotron Road, Berkeley, California 94720, United States.

*Corresponding author, E-mail: cdscown@lbl.gov

Abstract

Although ethanol remains the dominant liquid biofuel in the global market, there is a strong interest in high-energy density and low-hygroscopicity compounds that can be incorporated into gasoline at levels beyond the current ethanol blend wall. Isopentenol (3-methyl-3-buten-1-ol) is one of these promising advanced biofuels that is also an important precursor for isoprene (the main component of synthetic rubber). In this study, we model the production cost, greenhouse gas (GHG) emissions, and water footprint of biologically produced isopentenol, including the current state of the technology and the impact of potential improvements. We find that the minimum selling price of bio-based isopentenol, given the current state of technology demonstrated at bench-scale, is $5.14/L-gasoline equivalent, and the GHG footprint exceeds that of gasoline. However, bio-based isopentenol could reach $0.62/L-gasoline equivalent ($2.4/gal-gasoline equivalent (gge), just 5% above the 10-year average gasoline price) in an optimized future case where yield and other process parameters are pushed to near their theoretical limits. In this future case, isopentenol could achieve a GHG reduction of 90% relative to gasoline and a carbon abatement cost of $9.3/metric ton CO_{2e}. Reaching these goals will require dramatic improvements in isopentenol yield, near-100% recovery of ionic liquid used in pretreatment, and low-lignin, high- cellulose and hemicellulose biomass feedstocks.

Keywords: biomass sorghum; feedstock supply logistics; ionic liquid pretreatment; aerobic fermentation; biofuel

Introduction

Fuel ethanol production in the United States (U.S.) reached 165.3 million liters per day (1.04 million barrels per day) in May 2018, which equates to 11.8% of the total gasoline consumption of the country.[1] Unfortunately, with a limited number of flex-fuel vehicles and fueling stations available, and a maximum blending ratio of approximately 10 vol% for conventional vehicles (with a possible increase to 15%),[1,2] it is critically important to begin shifting production towards advanced biofuels that can be blended at higher ratios. Successful advanced fuels must avoid the challenges associated with ethanol's low energy density and high hygroscopicity.[2] Bio-derived fuels can range from alkanes and alkenes, which are indistinguishable from components of conventional gasoline, to more complex mixtures such as refined products derived from bio-crude.[2] Biological production of fuel compounds offers more precision and consistency than thermochemical routes, but theoretical yields of highly-reduced compounds are low because removal of oxygen in the form of water requires additional sugars to supply the necessary hydrogen (assuming no other source of hydrogen is utilized).[3] Producing oxygenated compounds with improved fuel properties relative to ethanol can help to avoid these yield penalties while still increasing the biofuel blend wall, although long lead times for getting new fuel blends approved will remain a challenge and must be addressed on a broader policy level.[4]

Mid-chain alcohols, such as isopentenol (3-methyl-3-buten-1-ol, also known as isoprenol), are attractive alternatives to ethanol due to several advantages including higher energy density, lower hygroscopicity and vapor pressure, and compatibility with the existing engines at higher blending ratios.[5–7] However, further research and development efforts are required to determine the most efficient blending ratio in existing engines. Isopentenol has a research octane number that, while not as high as ethanol, is higher than premium gasoline at 96.5.[8] The theoretically estimated lower and higher heating values (LHV and HHV) of isopentenol of 34.4 and 36.9 MJ/kg are 29 and 24 % higher than the corresponding values for ethanol, respectively.[9] It is also an important precursor of isoprene (the main component of natural rubber) and of flavor compounds (prenols and isoamyl alcohol esters), making it particularly flexible as a fuel or an intermediate for chemical/rubber production.[10] Although these properties and end uses make isopentenol a desirable product, a forward-looking evaluation is necessary to understand whether biological production of this target compound has the potential to achieve competitive costs and reduce greenhouse gas (GHG) emissions.

There are two different engineered metabolic pathways known that can be used to produce isopentenol in *Escherichia coli*: (i) amino acid production pathways utilizing 2-keto-acid intermediates, and (ii) isoprenoid biosynthesis pathways, such as mevalonate (MVA) pathway and non-mevalonate pathway (either methylerythritol 4-phosphate (MEP) or 1-deoxy-D-xylulose 5-phosphate (DXP) pathway).[10,11] In this study, we consider the mevalonate-dependent biosynthetic pathway because it has been demonstrated to achieve higher yields.[6,10] Compared to ethanol, the heating value-adjusted stoichiometric theoretical yield for isopentenol from glucose is roughly equivalent (40.9 g isopentenol/100 g-sugar, calculated using glucose as the sole source of required hydrogen and carbon,[12] which is 19.8% lower on an

unadjusted mass basis). The theoretical stoichiometric yield for isopentenol from xylose is essentially the same (40.9 wt%).The actual yield of isopentenol depends on metabolic pathways. For instance, the DXP pathway corresponds to a theoretical isopentenol yield of about 37.6 g/100 g-sugars.[9] Currently demonstrated yields are still well below theoretical, and these pathways require aerobic bioconversion, which adds cost and energy requirements relative to anaerobic fermentation. The remaining question is whether isopentenol production can be economically feasible and environmentally beneficial, and what yields must be achieved to reach key cost and GHG thresholds.

This study presents the first techno-economic analysis (TEA) and life-cycle inventories of GHG emissions and water use for a commercial-scale isopentenol production system considering bench-scale studies[13,14] conducted in recent years. The system is modeled using biomass sorghum as the feedstock because of farmers' familiarity with the crop (U.S. farmers currently grow forage sorghum),[15] the potential for biomass yields as high as 28 dry metric ton/ha,[16] potentially high carbohydrate content (as much as 70 wt%),[17] and drought tolerance.[18] This study considers a biocompatible choline-based ionic liquid (IL), cholinium lysinate ([Ch][Lys]) for pretreatment[19] A subsequent enzymatic hydrolysis process releases most of the hexose (C6) and pentose (C5) sugars. The process configuration is based on an integrated high-gravity (iHG) approach that minimizes costs and sugar losses.[20] Through our analysis, we are able to evaluate the current state of technology, identify possible bottlenecks, and provide research approaches most likely to improve future performance. We also show what is required to exceed the U.S. Department of Energy-established goal of $0.79/L-gasoline equivalent ($3/gal-gasoline equivalent (gge)), a more conservative target of $1.32/L-gasoline equivalent ($5/gge), and ≥ 60% reduction in the GHG emissions as compared to petroleum.[21]

Methods

Scope and System Overview

This study aims to assess the minimum selling price, life-cycle GHG emissions, and the life-cycle water footprint of biosynthetic isopentenol production. Results for the TEA are reported in $/L-gasoline equivalent and for LCA, the functional unit is 1 MJ-isopentenol (HHV) produced, at the biorefinery gate. These are selected to facilitate simple comparisons between volume-based fuel prices and per-MJ GHG emission factors used in the Renewable Fuel Standard (RFS) and Low Carbon Fuel Standard (LCFS). The 1 MJ functional unit presumes that the vehicle efficiency does not change appreciably for engines running on isopentenol blends relative to conventional gasoline; further engine testing is needed to confirm this assumption and U.S. Department of Energy-supported efforts to co-optimize future engine designs for biofuel blends are ongoing.[22] The system boundary includes all farm-level inputs and emissions, harvesting and logistics, and conversion to isopentenol, with boundaries ending at the biorefinery gate (i.e., isopentenol is ready to distribute for end use applications). This study does not include the impact of land use changes on the carbon footprint although the limited existing studies[23,24] suggest that biomass sorghum may have a large carbon sequestration potential on par with perennial crops such as

Miscanthus, likely because of its deep root system. Further collection of empirical data related to soil organic carbon sequestration during biomass sorghum cultivation across different land types and climatic conditions is required before this can confidently be included in net GHG estimates. Figure 1 depicts all the stages of the isopentenol production chain with their major monetary, material, and external energy inputs.

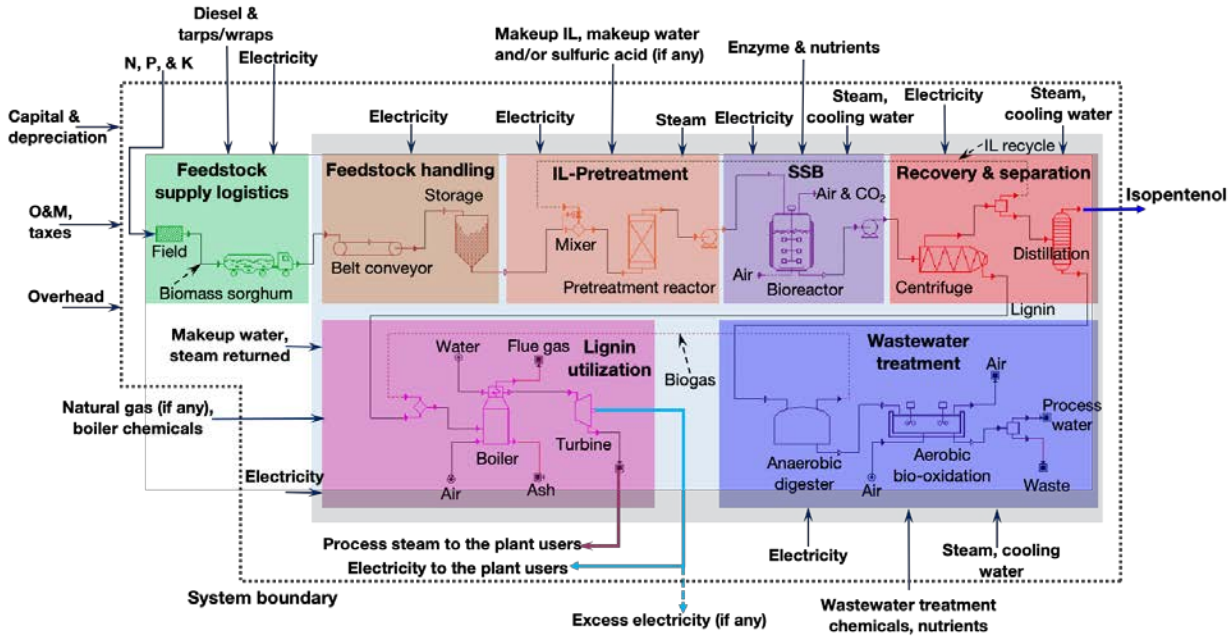

Figure 1. System boundary for TEA and LCA with selected process equipment. This figure illustrates cost, energy, and material inputs associated with the major isopentenol production stages (N: nitrogen, P: phosphorous, K: potassium, SSB: simultaneous saccharification and bioconversion).

Biorefinery Supply Chain and Process Model

Biomass Sorghum Supply System

We model the system using a hypothetical biorefinery sized to process the equivalent of 2000 bone dry metric tons (t) of biomass sorghum per day. Biomass sorghum contains about 60% moisture[25,26] at the time of harvest because of its limited ability to dry down[16] in the field. The biomass feedstock is assumed to be delivered directly from field to biorefinery by truck in the form of chopped biomass (at 40% moisture) and ensiled next to the biorefinery. A typical biomass harvest rate of 22 t/ha (10 tons/acre) is considered to determine biomass production and supply costs.[16] The feedstock supply radius is determined considering biomass yield, available land for sorghum cultivation around the biorefinery, and the road-winding factor (Supporting Information (SI)- Table S1), assuming a circular feedstock collection area where the biorefinery is located at the center of the circle. Although pelletizing biomass does reduce transportation costs, we find this to be impractical within a 95 km supply radius because of the additional energy required to dry down the chopped-biomass sorghum from 60% moisture content to 7-10%. Therefore, the direct transportation of the chopped biomass from the field to the biorefinery is selected for analysis in this study, which is valid for the feedstock supply

radius of 95 km (59 miles) complying the assumptions made in this study (SI-Table S1). A recent study illustrates the tradeoffs of several conventional and advanced feedstock supply scenarios for biomass sorghum including chopped (ensiled) biomass, bales, modules, and pellets.[27]

The biomass sorghum supply system encompasses five different processes: (1) biomass production, (2) biomass harvesting and loading into trucks, (3) transportation of chopped biomass to the biorefinery, and (4) unloading and storage at the biorefinery. The modeling assumptions and data are consistent with similar previous studies utilizing biomass sorghum[28–30] and other lignocellulosic feedstocks.[31,32] Briefly, biomass production includes establishment cost (includes machinery, labor, fuel and land rent), nutrient application (includes N, P, and K replacement due to the removal of biomass sorghum from the field), and herbicide/pesticide application. Biomass is harvested and chopped to the appropriate particle size with a forage harvester and transported directly to the biorefinery via truck. Due to the short harvesting window of 31.5 days,[33] on average, the chopped biomass is ensiled (stored) outside the biorefinery in a bunker silo covered with a tarp for the remainder of the year. The overall dry matter loss was assumed to be 14%, which is largely dependent on moisture content and the packing density in silo, as well as harvesting and handling losses.[34] More details on fertilizer, energy, and other material inputs are included in the SI-Tables S1 and S2.

Deconstruction and Bioconversion

The isopentenol production process is divided into six stages: (1) feedstock handling; (2) pretreatment; (3) hydrolysis and bioconversion; (4) recovery and separation; (5) wastewater treatment; and (6) onsite energy generation. These different stages along with material and energy inputs are shown in Figure 1. Unless otherwise indicated, our process models use assumptions consistent with the corn stover-to-ethanol process developed by National Renewable Energy Laboratory (NREL), [35–37] and similar previous TEA/LCA studies.[19,20,38] We created two distinct cases: baseline, which reflects the near-term state of technology, and optimal, which reflects long-term technological advancements. In the baseline case, the feedstock handling section entails the receiving, storage, and delivery of biomass to the pretreatment reactor. This stage includes truck unloading, conveying (belt conveyor), and short-term storage. The forage harvester can be adjusted to cut biomass to the required particle size of approximately 0.25 in.[35] to 1.5 in.,[36] which eliminates the need for further size reduction at the biorefinery. Pretreatment includes [Ch][Lys] pretreatment and subsequent pH adjustment with sulfuric acid. Table 1 summarizes the operating temperature, time, and the loading rates of biomass, IL, and sulfuric acid. Following the IL-pretreatment, the pretreated slurry is pumped to the simultaneous saccharification and bioconversion unit. Operating conditions for hydrolysis and bioconversion, including the enzyme loading rate, sugar yields, and isopentenol yield from sugars, are summarized in Table 1. After the hydrolysis and bioconversion, the IL and isopentenol are recovered in the subsequent recovery and separation process. This process includes centrifugation and ultrafiltration to remove solid particles,

followed by pervaporation to recover the IL,[39] and distillation and decantation to recover isopentenol. This study considers isopentenol and IL recovery rates of 95% and 97%, respectively, (Table 1) for the baseline scenario, which will require additional process demonstration at scale.

The liquid waste after recovery of the IL and isopentenol goes to the wastewater treatment unit and the solid waste (mainly lignin) is delivered to the boiler. The wastewater treatment section includes anaerobic digestion and aerobic treatment of wastewater. The anaerobic digestion generates biogas, which is subsequently delivered to the boiler. Both the lignin and biogas, and supplementary natural gas (where required) are used in the boiler to generate process steam, which is delivered to the steam turbine to generate electricity for the plant. The remaining steam from the turbine is used for process heat in the facility. The resulting process model provides detailed results for capital equipment, labor, and detailed mass and energy balances. Capital and operating cost parameters, as well as the estimation procedures, are consistent with the previously referenced NREL study[35] including a facility service life of 30 years, a biorefinery size of 2000 t dry biomass/day and annual operating hours of 7920 h (24 h/day and 330 days/year), internal rate of return of 10%, and income tax of 35%. All costs are scaled to 2018 dollars. In the baseline yield scenario (50% of stoichiometric theoretical yield, see Table 1), the facility produces 75.2 million liters of isopentenol/year (19.8 million gallons/year). The optimal case is configured similarly to the baseline biorefinery with a few key differences: 1) some yields and other metrics are improved, as reflected in Table 1; 2) a protic IL is used for pretreatment, eliminating the need for the pH adjustment step; 3) bioconversion is completed under micro-aerobic conditions. In this case, the shift to micro-aerobic conditions eliminates the need for any natural gas imports because net heat and electricity consumption is reduced below the total generated through the combustion of lignin and biogas.

Table 1. Major operating and process parameters used to develop process model and determine the required material, energy and cost[α]

Process parameters	Units	Baseline	Optimal	Process parameters	Units	Baseline	Optimal
Feedstock cost composition				***Aerobic Pathways***			
Feedstock cost	$/metric ton	101.8	60	Aeration rate[40–42]	VVM	1	N/A
Cellulose[17,43–49]	wt%	35.8	40	Power consumption[50]	kW/m^3	3	N/A
Hemicellulose[17,43–49]	wt%	22.9	27.4	Power dissipation to heat[50,51]	%	80	N/A
IL Pretreatment				***Micro-aerobic pathways***			
Solids loading rate[19,20,35]	wt%	30	30	Aeration rate[40,41,52,53]	VVM	0.35	0.2
IL-loading rate[20]	kg/kg-dry biomass	0.29	0.29	Power consumption[50]	kW/m^3	0.5	0.1
IL-cost[20,38]	$/kg	2	1	Power dissipation to heat[50,51]	%	40	30
Sulfuric acid loading[20,38]	kg-acid/kg-IL	0.2	0	***Isopentenol***[10,13,54]			
Sulfuric acid price[35–37]	$/kg	0.14	N/A	Fermentation time	h	72	36
Lignin to soluble lignin	wt%	65	65	Glucose conversion	wt%	20.45	36.81
Pretreatment time	h	3	3	Xylose conversion	wt%	20.45	36.81
Enzymatic hydrolysis							
Solids loading rate	wt%	20	30	**Recovery and separation**			
Enzyme loading rate	mg-protein/g glucan	20	7	Recovery of isopentenol (assumed[35])	wt%	95	97
Cellulose to glucose	wt%	84	95	IL recovery[19,20,55]	wt%	97	99
Xylan to xylose	wt%	80	90				
Hydrolysis time	h	72	72	**Lignin utilization**			
Enzyme price	$/kg-protein	5	5	Boiler chemicals price	$/kg	5	N/A
Bioconversion				Natural gas price	$/kg	0.2	N/A
Cost of corn steep liquor[35–37]	$/kg	0.1	0.1				
Cost of diammonium phosphate[35–37]	$/kg	1	1				

Yield Scenarios: Current Yield (CY) refers to current best-reported product yield (14% yield by mass from glucose and xylose), Baseline Yield (BY) refers to 50% of stoichiometric theoretical yield, Theoretical Yield (TY) refers to 100% of stoichiometric theoretical yield (40.9% yield by mass from glucose and xylose)

[α]Unless otherwise specified data summarized in this table were gathered from recent studies.[19,20,38] Parameters marked 'N/A' were not required for the given scenario.

Life-Cycle Greenhouse Gas and Water Footprints

Material and energy balances from the process model serve as inputs for a hybrid process-based/physical units-based input-output (IO) approach. We developed the IO matrix for all relevant direct and indirect inputs/outputs to compute the GHG emissions using data from widely used LCA databases[56–58] and previous literature. All data populating the model is selected based on representativeness of a U.S.-average case, with possible location-by-location variation captured in the probability distributions used for the Monte Carlo simulation. Individual data points are sourced from databases and studies deemed most reputable for each individual application, and wherever possible, multiple sources have been compared to ensure we are using the most accurate and representative values. In some cases where the data are not available, such as ionic liquid synthesis, we develop bottom-up process models to determine the required process chemicals, water, and energy inputs (vetted with industry experts). Our previous study[38] provides a detailed discussion of these methods and extensive

documentation of the data sources. To account for possible electricity exports from the biorefinery, we use system expansion assuming excess electricity offsets the average U.S. electricity mix. A GHG impact vector was constructed with direct emissions for each product/service included in the model and this was used to calculate the life-cycle GHG footprint.

We also calculate life-cycle water consumption and withdrawals associated with isopentenol production, including feedstock supply and the downstream conversion process. We consider water consumption and withdrawals embedded in material and energy inputs, as well as direct consumption and withdrawal of water at the biorefinery. Sorghum is assumed to be rain-fed only, so no irrigation is required. Water withdrawals refer to all water that is withdrawn from a freshwater source for use in a process/activity, while consumption is a subset of total withdrawals that only includes water evaporated or incorporated into the product (not immediately returned to the source). The primary difference occurs in open-loop cooling systems, which cycle through large volumes of water and evaporate only a small fraction. Previous studies provide detailed methods and discussion around water footprinting.[38,59] We use baseline material and energy input data to determine the baseline water consumption and withdrawals.

Scenario Analysis

Through scenario analysis, we are able to explore a solution space beyond what has been demonstrated in early-stage laboratory research. We have focused on a few key performance metrics that may be improved or altered to gauge their impact on final costs, GHG emissions, and water use. As discussed earlier, current biosynthetic isopentenol production in *E. coli* supports only aerobic pathways. However, the aerobic bioconversion is an energy-intensive process because of the need for forced aeration in the bioreactor.[50,51] This is a key challenge facing many biological routes to advanced biofuels. Shifting to micro-aerobic bioconversion pathways can reduce the required energy for the reactor and associated process equipment by reducing the required volume of air/oxygen supplied to the reactor and minimizing heat generated during the microbial conversion process.[50,51] Therefore, we evaluate a micro-aerobic pathway as a potential alternative scenario (assuming the same yield as the aerobic process can be accomplished); the actual isopentenol yield under micro-aerobic conditions is yet to be determined, and there may be a yield penalty.

In addition to comparing aerobic and micro-aerobic pathways, three different yield scenarios, including current yield, baseline yield (50% of stoichiometric theoretical yield from sugars), and theoretical yield, are evaluated in this study to demonstrate the importance of product yield in reducing the minimum selling price and GHG emissions. The best-reported yield at present is 14 g/100 g-sugar, which is referred to as the current yield (CY) scenario.[13] The estimated stoichiometric theoretical yield of isopentenol is 40.9 g/100 g-sugar.

Sensitivity and Uncertainty Analysis

We determine the most influential input parameters, for the minimum selling price, GHG emissions, and water use, by using the single point sensitivity analysis. Table S2 in the SI summarizes the minimum, maximum, and baseline values of each input parameter. The minimum and maximum values of these initial operating parameters are used to determine their influence on the minimum selling price, net GHG emissions, and water use. In addition to the sensitivity analysis, we determine the parameter uncertainty associated with the minimum selling price, GHG emissions, and water use. To represent uncertainty associated with the input parameters, we modeled initial operating parameters considering four different probability distribution functions: uniform, triangular, normal, and lognormal (SI-Table S2). The type of probability distribution for each parameter is selected based on data availability and the nature of input parameter (SI-Tables S1 and S2). We used 5000 Monte Carlo runs to determine the probability distributions for the results.

Results and Discussion

Minimum Selling Price of Isopentenol

For the baseline scenario (50% of stoichiometric theoretical yield from sugars, and process parameters further outlined in Figure 1), the estimated minimum selling price at the biorefinery gate is $3.5/L-gasoline equivalent. This price is 6 times greater than the 10-year average gasoline price at the refinery gate of $0.59/L.[60] Figure 2-a shows the importance of the product yield, absent any other improvements beyond the baseline scenario. Doubling the isopentenol yield to its stoichiometric theoretical maximum reduces its selling price by 49%. The impact on price can be even more dramatic when combined with selection of a feedstock with higher hemicellulose and cellulose content (SI-Figure S7-a). Across the different yield scenarios, the hydrolysis and bioconversion unit is the single largest contributor to the minimum selling price (accounting for 26% in the baseline scenario). Within that unit operation, process chemicals (enzymes and nutrients) and electricity required (air supply and reactor operations) are the primary expenses. Feedstock supply is the next largest cost component at 23% of the total minimum selling price. Delivered sorghum feedstock costs are primarily driven by on-field nutrient replacement (fertilizer application-SI-Table S1) and biomass transportation from the field to the biorefinery (SI-Figures S1 and S2). Although this study does not consider any specific locations, we note that siting biorefineries in areas where a large fraction of surrounding land is dedicated to feedstock production (thus decreasing transportation distances) and minimizing fertilizer application can reduce these costs.

Following feedstock supply and bioconversion, onsite energy generation, recovery and separation, and pretreatment are the next largest contributors to the minimum selling price, accounting for 20, 15, and 10%, respectively (Figure 2-a). Costs broken out by capital and operating expenditures are provided in SI-Figure S1 and contributions to minimum selling price are shown in Figure S2. Although onsite energy generation is a major contributor, the single

largest cost contributor is the boiler, which is required to produce process steam regardless of whether biogas and lignin are utilized onsite. Although we assume all biogas and lignin is combusted, regionally-varying grid electricity prices and values for biogas may incentivize some biorefinery owners to generate less energy onsite. Figure 2-b, c, and d show that net electricity sales to the grid decrease as yield increases. This decrease is owed to the smaller amount of unutilized sugars and other organic matter flowing to the on-site anaerobic digester, where biogas is generated for on-site heat and electricity generation. Therefore, as product yield increases, on-site energy production decreases.

In addition to improving product yield, switching from an energy-intensive aerobic bioconversion process to a micro-aerobic process is a promising avenue to reducing the minimum selling price, assuming the same yield can be maintained. Moving to a micro-aerobic bioconversion pathway reduces the minimum selling price by 14% compared to aerobic (Figure 2-a). This is because the micro-aerobic process requires less energy to supply air and agitation for the reactor, and less cooling water to maintain a constant temperature in reactor as this process generates less heat from microbial activities. These operating conditions reduce the operating cost for the bioconversion stage, which is key to minimizing the overall selling price of isopentenol. The lowest achievable minimum selling price in this case can be further cut in half by introducing additional feedstock and process improvements that comprise the optimal case (OP), on top of a micro-aerobic process at 90% of theoretical yield, as outlined in Table 1.

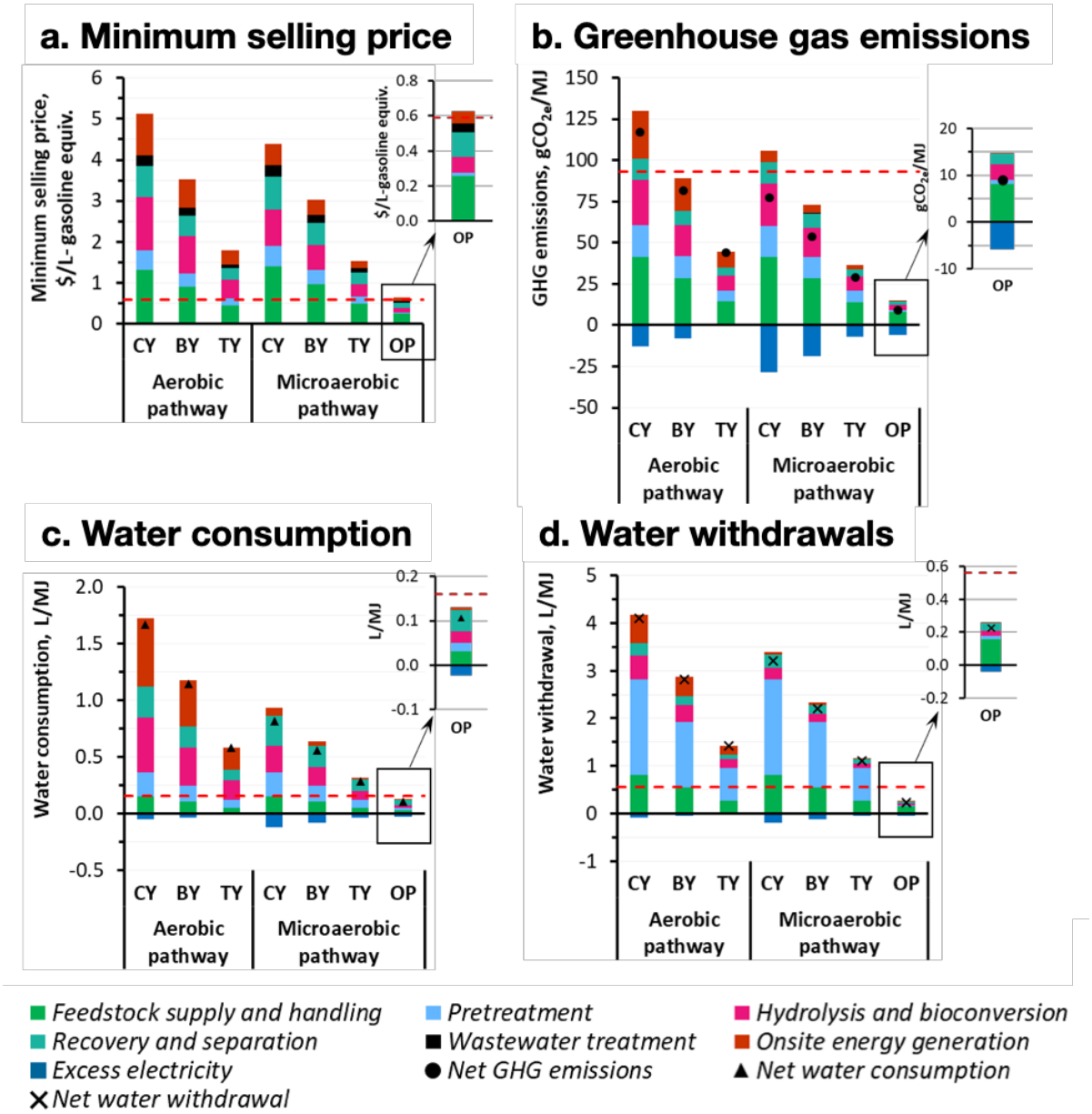

Figure 2. Minimum selling price, GHG emissions, and water footprint under different yield scenarios and the optimal future case. Horizontal dashed lines refer to gasoline baseline values: (a) 10-year (2008-2017) average refinery-gate price \$0.59/L;[60] (b) 93 gCO_{2e}/MJ (b);[38] (c) 0.16 L water consumed/MJ;[38] (d) 0.56 L water withdrawn/MJ.[38] Sensitivity bars (b) show the impacts of direct and indirect land use change. See Table 1 and SI-Figure S13 for the product yields considered for more detail on the baseline case, optimal case (OP), and the different yield scenarios: current yield (CY); baseline yield (BY); and theoretical yield (TY). The sensitivity bars (b) represent the GHG emissions impacts from land use changes.

Variations in the IL and enzyme loading rates, and recovery of IL (which reduces the required quantity of makeup IL), are key cost drivers; specifically, the IL loading and recovery rates are

the next most influential parameters after isopentenol yield and biomass total carbohydrate content (SI-Figure S3). Feedstock supply cost is another important parameter, which largely depends on the required nutrient, biomass yield, and available sorghum farming land around the biorefinery. Feedstock costs will, of course, also depend on local market conditions and prices are likely to fluctuate based on local supply and demand. Energy consumption by bioreactors, retention time, and solids loading rate are other key parameters, all of which are summarized in SI-Figure S3. These parameters either influence the selling price by altering the quantity of isopentenol (such as sugar yield and isopentenol recovery) or by varying the required capital and operating costs (e.g. solids loading rate and retention time vary size/quantity of process equipment and the required utilities).

We assume that, once the production process is optimized through future research and development efforts, the uncertainty associated with the minimum selling price will be reduced (Figure 3-a). Uncertainty analysis considering variability present in several input parameters (Table 1 and SI-tables S1 and S2) results a positively skewed probability distribution for the current, baseline, and optimal minimum selling prices (Figure 3-a). Feedstock supply, pretreatment, and SSB stages are the primary contributors to this uncertainty (SI-Figures S9).

Life-Cycle Greenhouse Gas Emissions

The net GHG footprint of isopentenol in the baseline scenario (50% of stoichiometric theoretical isopentenol yield) is 81 gCO_{2e}/MJ (Figure 2-b). While this GHG footprint does achieve a 13% reduction relative to conventional gasoline, it does not meet the emissions reduction target set by the Renewable Fuel Standard (RFS) for cellulosic biofuels. Two broad strategies can be employed to reduce the GHG footprint: (i) increase product yields while keeping key inputs constant and (ii) reduce emissions-intensive inputs, such as fertilizer and fossil fuels. Figure 2-b depicts the contribution to the overall GHG emissions from each stage of the isopentenol production chain. The sorghum biomass supply is the major contributor to the net GHG emissions, accounting for 35% of the total in the baseline scenario (not including direct and indirect land use change impacts). Nitrogenous fertilizer application, including upstream fertilizer manufacturing and on-farm N_2O emissions after application, and the combustion of diesel for transportation and field operations (harvesting and collection) are the drivers of emissions. Onsite energy generation at the biorefinery, hydrolysis and bioconversion, pretreatment, and recovery and separation are next largest contributors to the net GHG emissions, accounting for 24, 23, 16, and 11%, respectively. GHG emissions from these downstream processes are primarily due to process chemicals (enzymes and ILs), supplemental fuel needs (natural gas), and cooling/chilled water. These emissions can be reduced by lowering IL loading rates, improving the energy efficiency of the overall process, selecting biocompatible ILs that do not require pH adjustment, and switching from an aerobic to micro-aerobic bioconversion process. Utilizing process steam and electricity generated

onsite using lignin, biogas from wastewater treatment facility, and supplemental natural gas as needed is important for minimizing GHG emissions. However, this practice does have economic downsides as the solids boiler and turbogenerator are capital-intensive and grid electricity can be purchased at relatively low cost in many regions of the U.S.[61]

Figure 2-b demonstrates two specific avenues to reduce GHG emissions without negatively impacting the economics: (i) by improving product yield; and (ii) by switching from energy-intensive aerobic to a micro-aerobic bioconversion process. Both of these strategies require additional research and development. If the product yield is increased from the currently-demonstrated yield to maximum theoretical yield (see Table 1), the net GHG emissions of isopentenol can be reduced from 117 to 44 gCO_{2e}/MJ. Notable in Figure 2-b is the decrease in net electricity exports as product yield increases. This decrease in electricity exports occurs because, as sugars are more efficiently converted to isopentenol, there is less residual organic matter sent to the wastewater treatment unit, and thus less biogas available for onsite electricity generation. Shifting to a micro-aerobic bioconversion pathway further reduces the net GHG footprint to 29 gCO_{2e}/MJ because of the dramatic reduction in onsite energy use and resulting reduction in supplemental natural gas requirements (Figure 2-b).

The soil carbon sequestration potential of biomass sorghum reported in the DOE Billion-Ton study is striking in that it is larger than other bioenergy crops, including perennial grasses.[15] However, the soil organic carbon gain with biomass sorghum farming in cropland/pasture land presented in the DOE Billion-Ton study[15] is based on only a limited number of counties and to our knowledge there are not many supporting studies in the scientific literature. This is an area in need of additional research to improve GHG flux estimates for sorghum cultivation on converted agricultural and pastureland. Additionally, the indirect land use change values are also in need of further study and refinement in future studies, as the only literature values available are based on grain sorghum rather than forage/biomass sorghum. This issue is further complicated because some sorghum types are considered "all-purpose" and may be used for either grain or silage.

All other input parameters that alter the quantity of isopentenol and the required utilities influence the overall GHG emissions to varying degrees, as indicated in SI-Figure S4. Figure S7-b highlights the importance of isopentenol yield and total carbohydrates in the feedstock to the GHG emissions over a range of expected values. We find that electricity required for the aerobic-bioconversion unit (mainly to supply air and agitation) is a driving factor for emissions because it increases onsite energy demand beyond what can be supplied using only biogas and lignin produced on-site, and we assume natural gas and U.S. average grid electricity are consumed as needed. Therefore, switching from aerobic to micro-aerobic process is crucial for the mitigation of GHG emissions. An alternative option for minimizing emissions is to procure supplemental electricity from renewable resources such as wind, solar, or biogas from nearby

facilities. Facilities located in grid regions with less carbon-intensive electricity mixes are also at a relative advantage.

Variabilities in these key input parameters, including nutrient and chemical inputs at the farm and biorefinery, (SI-Tables S1, S2, and S3) result in positively skewed probability distributions for net GHG emissions (Figure 3-b). Input parameters associated with feedstock supply, pretreatment, and SSB are the primary contributors to this uncertainty (SI-Figure S10). Variations in the required nutrient, biomass yield, and available sorghum farming land are the major source of uncertainties for feedstock supply. The large uncertainty in biomass pretreatment is due to the large uncertainty present in IL recovery (which is so far based on theoretical system performance), biomass compositional quality (cellulose, hemicellulose, and lignin), and sugar yield. The uncertainty associated with isopentenol yield, enzyme loading rate, energy consumption by reactors and retention time are sources of uncertainties for SSB. Further research and scale-up efforts can narrow the probability distributions for these parameters over time and reduce overall uncertainty in the results (Figure 3-b).

Life-Cycle Water Footprint

Life-cycle water consumption and withdrawals for the entire isopentenol production chain under different scenarios are shown in Figures 2-c and 2-d, respectively. Switching from an aerobic to micro-aerobic process reduces water consumption and withdrawals by 51 and 22%, respectively. The water footprint of the onsite energy generation process is responsible for the large difference in water use between aerobic and micro-aerobic bioconversion pathways. Lower onsite electricity needs reduce the required size of the turbine and evaporative losses, as the steam turbine is responsible for 52% of the total cooling water evaporation[35] at the plant. Figures 2-c and 2-d also depict a large difference between water consumption and water withdrawals for pretreatment stage. This is primarily due to the use of sulfuric acid; manufacturing sulfuric acid requires substantial water withdrawals (66 L water withdrawn per kg of sulfuric acid produced vs. 5 L water consumed/kg sulfuric acid).[38] Sulfuric acid is used for pH adjustment, which can be eliminated by using a biocompatible protic IL,[19] that does not require pH adjustment before hydrolysis. Phosphorus manufacturing is also water withdrawal-intensive (9 times greater than its water consumption), and accounts for most of the difference between withdrawals and consumption for feedstock supply.[38] Apart from above major differences, both water consumption and water withdrawals are similar for other life-cycle stages of isopentenol production process (Figures 2-a and 2-b).

For the baseline scenario, the relative sensitivity of water consumption and withdrawals to variations in different input parameters are presented in SI-Figures S5 and S6, respectively. Isopentenol yield from sugars and the quality of biomass feedstock (total carbohydrate content) are the most influential to both water consumption and withdrawals per unit of isopentenol produced. Figures S8-a and S8-b illustrate their impacts on the water footprints considering their potential ranges. Electricity required for bioreactor operation, and

bioconversion time alter on-site energy generation and thus impact both water consumption and withdrawals. Evaporative losses of water from the cooling tower and turbine, as well as the moisture retained in solid waste and lignin, are responsible for the direct water consumption and withdrawals at the biorefinery (a negligible amount is also retained in the product as a result of the hydrolysis step). Agricultural nutrient inputs (N, P, and K) are more important for water withdrawals than water consumption because their production process, as with sulfuric acid, requires far larger water withdrawals relative to the amount consumed.[38] Apart from sulfuric acid, other process chemicals, including ILs and enzymes contribute to the water footprint of the downstream conversion process. Thus, the water footprint can be reduced by increasing IL-recovery and by reducing IL and enzyme loading rates (assume sugar yields can be maintained).

Strategies for reducing cost and GHG emissions are also central to improving water use efficiency and reducing uncertainty (Figures 3-c and 3-d). The current water consumption and withdrawals under aerobic pathways of 1.67 and 4.10 L/MJ are 10 and 7 times, respectively, higher than gasoline (Figures 2-c and 2-d). Pushing product yield toward the maximum theoretical yield and switching to microaerobic conversion pathways reduces the water consumption and withdrawals for isopentenol production to 0.29 and 1.11 L/MJ, respectively (Figures 2-c and 2-d). For comparison, the previous study on cellulosic ethanol production using an IL-based process[38] reported the water consumption and withdrawals in the range of 0.2-0.4 and 0.4-1.2 L/MJ, respectively. These results are comparable with the higher-yield, microaerobic conversion scenarios for isopentenol; however, these water footprints are still about 2-fold higher than the water footprint of gasoline (as is generally the case for biofuels, even without feedstock irrigation).

Future Performance Targets and Greenhouse Gas Emissions Mitigation Cost

In this study, we demonstrate that improving product yield to near the theoretical maximum is essential to reduce the minimum selling price, GHG emissions, and water footprint of isopentenol. Biological constraints limit the maximum possible theoretical yield, so we consider an optimal isopentenol yield of 36.8 wt% from convertible sugar, which is 90% of the stoichiometric theoretical yield. This is close to the DXP pathway-dependent maximum isopentenol yield of 37.6 wt% reported in a previous study, and would require extensive metabolic engineering research and development efforts to achieve.[9] There are other potential strategies for achieving high yields; for example, host microbes could be engineered to utilize other plant-derived intermediates as a hydrogen source, which would enable yields beyond the stoichiometric maximum discussed here.[62] However, yield improvements alone are not sufficient to achieve any of the minimum selling price targets,[21] the RFS GHG reduction target, nor a water footprint comparable with gasoline. With this assumed optimal yield along with the baseline values for other process parameters (Tables 1 and S2), the minimum selling price and GHG emissions are reduced to \$2.0/L-gasoline equivalent (\$7.6/gge) and 48.2 gCO_{2e}/MJ, respectively. In contrast, the RFS requires 37.2 gCO_{2e}/MJ or less (60% reduction relative to

gasoline). Detailed process parameters and their values are presented in Table 1. Additionally, improving the product yield from the baseline value to the optimal reduces the water consumption and withdrawals to 0.64 and 1.57 L/MJ, respectively. These are large reductions relative to the baseline results (Figure 2); however, further efforts are required to hit the targeted selling prices, the RFS GHG emissions mitigation target, and water footprints more comparable to gasoline.

To explore additional feedstock and process improvements that can help reach the target selling prices, GHG footprint, and water footprints, we conducted a single-point sensitivity analysis (see Figures S3 to S6). We find that a high-quality biomass feedstock (total carbohydrates >70 wt%) is central to the optimal future case, resulting in lower minimum selling price, GHG emissions, and water footprint. Research focused on modifying the secondary cell wall to increase cellulose and hemicellulose content, and/or screening existing varieties for these traits while maintaining high yields is critical to achieving cost and environmental targets. Sustainable agricultural practices with reduced application of nutrients (particularly nitrogen) and alternative feedstock harvesting machinery and trucks, reliant on lower-carbon energy sources including electricity or natural gas are required to reduce emissions associated with the feedstock supply system. For sorghum specifically, avoiding high moisture content at the time of harvest is essential to minimizing dry matter losses (SI-Table S1) or degradation of biomass quality of over the time. Additionally, efficient deconstruction methods are required to release >90% of the sugars from the feedstock. IL-pretreatment has the potential to liberate sugars at >90% yield from a variety of biomass sources, although further research is required to reduce the IL loading rate (<10 wt%-based on the total slurry), to increase IL recovery (>97 wt% of the initial IL), while maintaining high sugar yields. The pH adjustment step can be eliminated by switching to biocompatible protic ILs.[19,55] Saccharification efficiency must also improve with lower enzyme loading rates (<10 mg protein/g-glucan). Improving product yield while switching from aerobic to microaerobic bioconversion conditions is particularly effective at reducing the GHG footprint. Achieving all the optimal process conditions discussed above (also outlined in Table 1) reduces the minimum selling price, the overall GHG emissions, water consumption, and water withdrawals of isopentenol to \$0.62/L-gasoline equivalent (\$2.3/gge), 8.9 gCO_{2e}/MJ, 0.11 L/MJ, and 0.23 L/MJ, respectively. These values can be thought of as near-theoretical minima for a very mature supply chain and conversion process. Further detailed discussion about potential future research pathways is available in a recent review article.[61]

In reality, efforts to optimize the feedstock and conversion process for minimized costs, GHG emissions, and water use will not result in guaranteed single-point results but rather a range depending on a host of technological, time-dependent, and region-dependent variations beyond the control of researchers. Figure 3 shows the results of a Monte Carlo simulation for the Current, Baseline, and Optimal scenarios. There is a non-zero, but low, likelihood of

achieving the optimal selling price of $0.62/L-gasoline equivalent. However, Figure 3 indicates that there is an approximately 10% likelihood of achieving the targeted selling price of isopentenol of $0.79/L ($3/gge) and water footprint for isopentenol below the gasoline baseline. With potential future improvements in the optimal scenario (see details in Figure S13), the GHG emissions from isopentenol production have a 70% likelihood of reaching a 60% or greater reduction relative to gasoline (Figure 3-b) and there is more than 60% likelihood of achieving water withdrawals below the gasoline baseline (Figure 3-d).

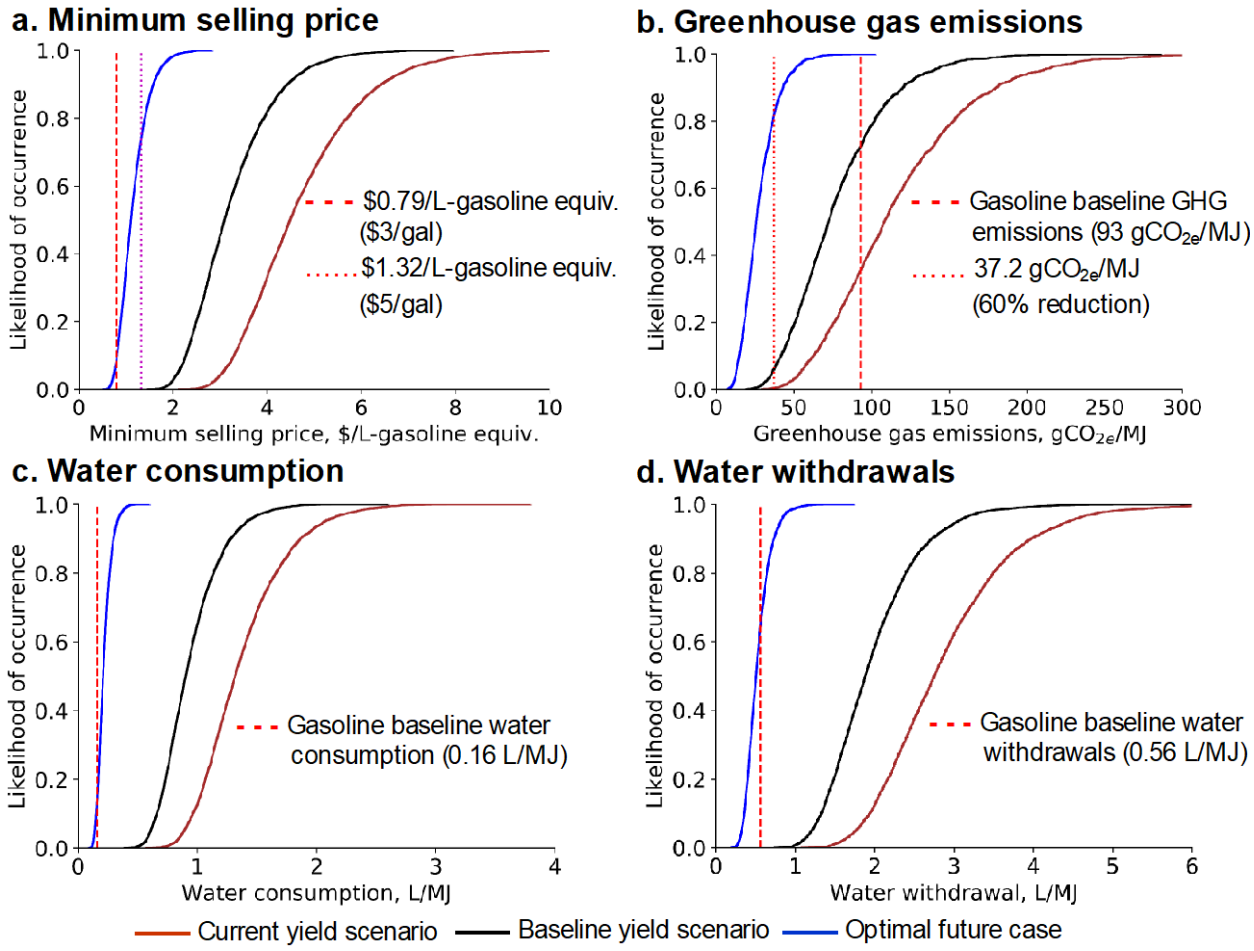

Figure 3. Cumulative probability distributions for minimum selling price (a), GHG emissions (b), water consumption (c), and water withdrawal (d) under current and baseline yield scenarios and optimal future cases.

Combining life-cycle GHG emissions results with the estimated MSP allows us to calculate the cost of carbon mitigation, which can be interpreted as the price that would need to be placed on a metric ton of CO_{2e} emissions in order to reach cost parity with gasoline. This makes it possible to compare bio-based isopentenol with a wider range of other technologies based on the cost-effectiveness of emissions mitigation. At currently-demonstrated yields and process

conditions, isopentenol has a larger GHG footprint than gasoline; an aerobic bioconversion pathway at 14 g of isopentenol yielded per 100 g-sugar generates 26% more net fossil GHG emissions than gasoline. Potential microaerobic pathways at the same currently-demonstrated yield reduces the overall GHG emissions by 17% relative to gasoline but the prohibitively high cost results in a very high GHG mitigation cost of \$6,363/t-CO_{2e} avoided (for microaerobic pathways). In the baseline scenario (50% of theoretical yield and aerobic conditions), there is an approximately 20% chance of GHG emissions reductions relative to gasoline (Figure 4-a).

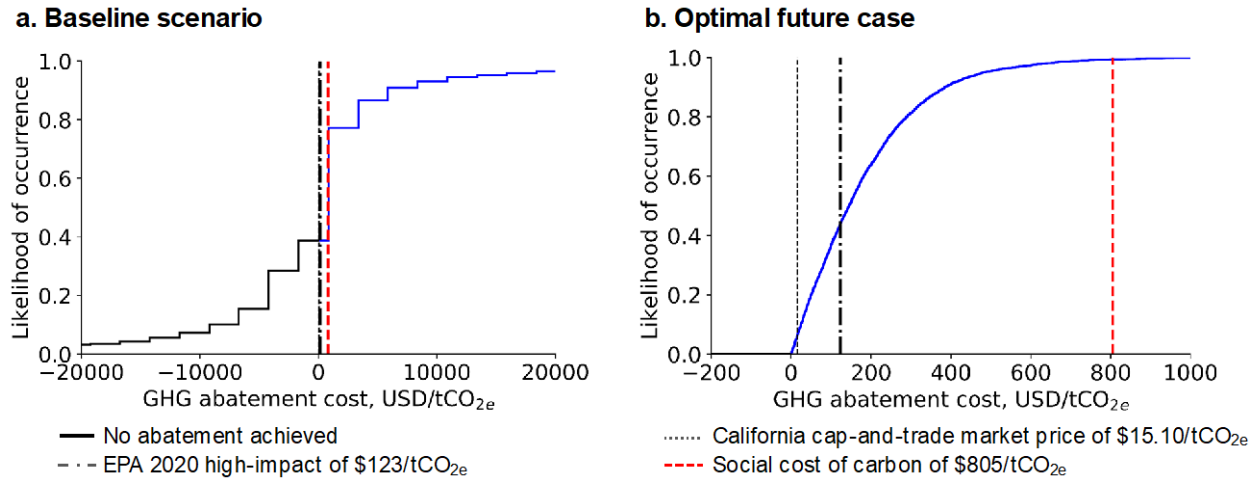

Figure 4. Likelihood of achieving different GHG mitigation costs for isopentenol under the baseline scenario (a) and the optimal future case (b) (Table 1 and SI- Figure S13). 'USD' refers to the United States Dollar.

When the product yield is pushed to the maximum theoretical value while holding all other parameters at their baseline values, the net GHG emissions are reduced by 54.2-68.7%, depending on the conversion pathways, resulting in a carbon mitigation cost of \$363-612/t-CO_2 avoided. Additional research and development efforts leading to the optimal scenario discussed earlier can achieve a 90% GHG emissions reduction relative to gasoline and a carbon mitigation cost to \$9.3/t- CO_{2e} avoided. For comparison, California's cap-and-trade value is \$15.10/t-CO_{2e} and this does not account for the additional value of RFS renewable identification numbers (RINS) or Low Carbon Fuel Standard (LCFS) credits.[61] This is a very encouraging result, although it should be thought of as a theoretical minimum value rather than an expected value (about 5% certainty, Figure 4-b). At GHG mitigation values closer to the EPA 2020 high-impact value of \$123/t-CO_{2e}, an optimized isopentenol production process has a nearly 50% likelihood of being competitive. These results suggest that, although extensive further research and development are required, including large improvements in isopentenol yield and titer, bio-based isopentenol has potential to be an economically attractive gasoline blendstock and compete with other renewables on the basis of carbon mitigation cost.

For Table of Contents Use Only

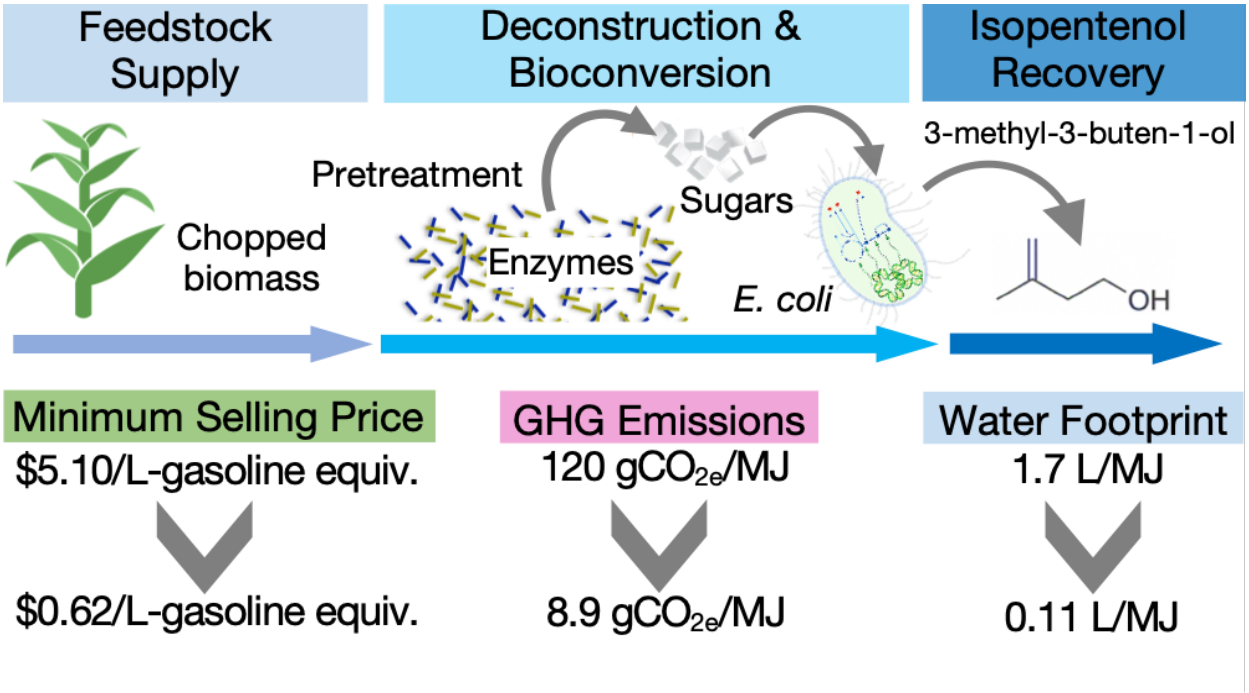

TOC Synopsis:

Bio-derived isopentenol fuel can reduce GHG emissions with competitive costs at commercially-relevant titers, rates, and yields.

Disclosures

The authors declare no competing financial interest.

Supporting Information

Supporting information includes data associated with feedstock supply logistics, and biochemical conversion process. The file also includes detailed uncertainty analysis results for each stage of supply chain.

Acknowledgements

This work was part of the DOE Joint BioEnergy Institute (http:// www.jbei.org) supported by the U.S. Department of Energy, Office of Science, Office of Biological and Environmental Research, through contract DE-AC02-05CH11231 between Lawrence Berkeley National Laboratory and the U.S. Department of Energy. The United States Government retains and the publisher, by accepting the article for publication, acknowledges that the United States Government retains a non-exclusive, paid-up, irrevocable, world-wide license to publish or reproduce the published form of this manuscript, or allow others to do so, for United States Government purposes.

References

(1) U.S. Energy Information Administration (EIA). U.S. fuel ethanol production continues to grow in 2017. *U.S. Energy Information Administration, Washington, DC*, **2018**; https://www.eia.gov/todayinenergy/detail.php?id=32152 (accessed January 22, 2019).

(2) Eagan, N. M.; Kumbhalkar, M. D.; Buchanan, J. S.; Dumesic, J. A.; Huber, G. W. Chemistries and Processes for the Conversion of Ethanol into Middle-Distillate Fuels. *Nat. Rev. Chem.* **2019**, 3, 223-249.

(3) Blanch, H. W. Bioprocessing for biofuels. *Curr. Opin. Biotechnol.* **2012**, *23* (3), 390–395, DOI 10.1016/j.copbio.2011.10.002.

(4) Lade, G. E.; Cynthia Lin Lawell, C. Y.; Smith, A. Designing Climate Policy: Lessons from the Renewable Fuel Standard and the Blend Wall. *Am. J. Agric. Econ.* **2018**, *100* (2), 585–599.

(5) Shi, J.; George, K. W.; Sun, N.; He, W.; Li, C.; Stavila, V.; Keasling, J. D.; Simmons, B. A.; Lee, T. S.; Singh, S. Impact of pretreatment technologies on saccharification and isopentenol fermentation of mixed lignocellulosic feedstocks. *BioEnergy Res.* **2015**, *8* (3), 1004–1013, DOI 10.1007/s12155-015-9588-z.

(6) George, K. W.; Chen, A.; Jain, A.; Batth, T. S.; Baidoo, E. E. K.; Wang, G.; Adams, P. D.; Petzold, C. J.; Keasling, J. D.; Lee, T. S. Correlation analysis of targeted proteins and metabolites to assess and engineer microbial isopentenol production. *Biotechnol. Bioeng.* **2014**, *111* (8), 1648–1658, DOI 10.1002/bit.25226.

(7) Liu, H.; Wang, Y.; Tang, Q.; Kong, W.; Chung, W.-J.; Lu, T. MEP pathway-mediated isopentenol production in metabolically engineered Escherichia coli. *Microb. Cell Fact.* **2014**, *13* (1), 135, DOI 10.1186/s12934-014-0135-y.

(8) Mack, J.H., Rapp, V.H., Broeckelmann, M., Lee, T.S., Dibble, R.W. Investigation of

biofuels from microorganism metabolism for use as anti-knock additives. Fuel, **2014**, *117*, 939–943, DOI 10.1016/j.fuel.2013.10.024.

(9) Klein-Marcuschamer, D.; Blanch, H. W. Survival of the fittest: an economic perspective on the production of novel biofuels. *AIChE J.* **2013**, *59* (12), 4454–4460, DOI 10.1002/aic.14245.

(10) Kang, A.; George, K. W.; Wang, G.; Baidoo, E.; Keasling, J. D.; Lee, T. S. Isopentenyl diphosphate (IPP)-bypass mevalonate pathways for isopentenol production. *Metab. Eng.* **2016**, *34*, 25–35, DOI 10.1016/j.ymben.2015.12.002.

(11) Withers, S. T.; Gottlieb, S. S.; Lieu, B.; Newman, J. D.; Keasling, J. D. Identification of isopentenol biosynthetic genes from Bacillus subtilis by a screening method based on isoprenoid precursor toxicity. *Appl. Environ. Microbiol.* **2007**, *73* (19), 6277–6283, 10.1128/AEM.00861-07.

(12) Dunlop, M. J.; Dossani, Z. Y.; Szmidt, H. L.; Chu, H. C.; Lee, T. S.; Keasling, J. D.; Hadi, M. Z.; Mukhopadhyay, A. Engineering Microbial Biofuel Tolerance and Export Using Efflux Pumps. *Mol. Syst. Biol.* **2011**, *7* (1), 1-7; 10.1038/msb.2011.21.

(13) Kang, A.; Mendez-Perez, D.; Goh, E.-B.; Baidoo, E.; Wang, G.; Beller, H.; Keasling, J.; Lee, T. Optimization of the IPP-bypass mevalonate pathway and fed-batch fermentation for the production of isoprenol in *Escherichia coli*. 2019. Metabol Eng. Under Review.

(14) Lee, T. S.; Kang, A. Novel Host Cells and Methods for Producing Isopentenol from Mevalonate. Google Patents, US 10273506B2,March 22, 2018.

(15) Cui, X.; Kavvada, O.; Huntington, T.; Scown, C. D. Strategies for Near-Term Scale-up of Cellulosic Biofuel Production Using Sorghum and Crop Residues in the US. *Environ. Res. Lett.* **2018**, 13, 1-9, 10.1088/1748-9326/aae6e3.

(16) U.S. Department of Energy (DOE). 2016 Billion-Ton Report: Advancing Domestic Resources for a Thriving Bioeconomy. U.S. Department of Energy, Washington, DC, 2016; https://www.energy.gov/sites/prod/files/2016/12/f34/2016_billion_ton_report_12.2.16_0.pdf (accessed January 22, 2019).

(17) Theerarattananoon, K.; Wu, X.; Staggenborg, S.; Propheter, J.; Madl, R.; Wang, D. Evaluation and Characterization of Sorghum Biomass as Feedstock for Sugar Production. *Trans. ASABE* **2010**, *53* (2), 509–525, DOI 10.13031/2013.29561.

(18) U.S. Department of Energy (DOE). Studying Drought Tolerance in Sorghum. U.S. Department of Energy, Washington, DC, **2015**; https://jgi.doe.gov/studying-drought-tolerance-sorghum/(accessed July 18, 2019).

(19) Sun, J.; Konda, N. M.; Parthasarathi, R.; Dutta, T.; Valiev, M.; Xu, F.; Simmons, B. A.; Singh, S. One-pot integrated biofuel production using low-cost biocompatible protic ionic liquids. *Green Chem.* **2017**, *19* (13), 3152–3163, DOI 10.1039/C7GC01179B.

(20) Xu, F.; Sun, J.; Konda, N. M.; Shi, J.; Dutta, T.; Scown, C. D.; Simmons, B. A.; Singh, S. Transforming biomass conversion with ionic liquids: process intensification and the development of a high-gravity, one-pot process for the production of cellulosic ethanol. *Energy Environ. Sci.* **2016**, *9* (3), 1042–1049, DOI 10.1039/C5EE02940F.

(21) U.S. Department of Energy (DOE). Bioenergy Technologies Office Mission and Goals Technology Development Timeline and Key Activities. U.S. Department of Energy,

Washington, DC, **2016**; https://www.energy.gov/sites/prod/files/2016/03/f30/mypp_beto_march2016_2.pdf (accessed January 22, 2019).

(22) U.S. Department of Energy (DOE). Co-Optimization of Fuels & Engines : FY18 Year in Review. U.S. Department of Energy, Washington, DC, 2019; https://www.osti.gov/biblio/1542263 (accessed August 19, 2019).

(23) U.S. Department of Energy (DOE). 2016 Billion-Ton Report, Volume 2: Environmental Sustainability Effects of Select Scenarios from Volume 1. U.S. Department of Energy, *Washington, DC*, **2016**; https://www.energy.gov/eere/bioenergy/downloads/2016-billion-ton-report-volume-2-environmental-sustainability-effects (accessed January 22, 2019).

(24) Dou, F.; Wight, J. P.; Wilson, L. T.; Storlien, J. O.; Hons, F. M. Simulation of biomass yield and soil organic carbon under bioenergy sorghum production. *PLoS One* **2014**, *9* (12), e115598, DOI 10.1371/journal.pone.0115598.

(25) Billa, E.; Koullas, D. P.; Monties, B.; Koukios, E. G. Structure and composition of sweet sorghum stalk components. *Ind. Crops Prod.* **1997**, *6* (3), 297–302, DOI 10.1016/S0926-6690(97)00031-9.

(26) Borden, D. Effect of Harvest Dates on Biomass Accumulation and Composition in Bioenergy Sorghum Effect of Harvest Dates on Biomass Accumulation and Composition in Bioenergy Sorghum. Texas A&M University, MS Thesis, **2011**; http://oaktrust.library.tamu.edu/bitstream/handle/1969.1/ETD-TAMU-2011-12-10401/BORDEN-THESIS.pdf?sequence=2 (accessed January 22, 2019).

(27) Baral, N.R.; Putnam, D.; Dahlberg, J.; Scown, C.D. Biomass Sorghum Supply Systems for Advanced Biofuel Production. Genomic Sciences Program Annual Principal Investigator (PI) Meeting, U.S. Department of Energy, *Washington, DC*, **2019**; https://genomicscience.energy.gov/pubs/2019abstracts/abstracts/Keasling_Baral.pdf (accessed April 15, 2019).

(28) Sokhansanj, S.; Webb, E.; Turhollow Jr, A. F. *Development of the integrated biomass supply analysis and logistics model (IBSAL)*; Oak Ridge National Laboratory (ORNL), 2008.

(29) Turhollow, A. The economics of energy crop production. *Biomass and Bioenergy* **1994**, *6* (3), 229–241 DOI 10.1016/0961-9534(94)90077-9.

(30) Oak Ridge National Laboratory (ORNL). *Cost Methodology for Biomass Feedstocks : Herbaceous Crops and Agricultural Residues.* Oak Ridge National Laboratory, Oak Ridge, TN, **2009**; https://digital.library.unt.edu/ark:/67531/metadc933499/m1/1/ (accessed January 22, 2019).

(31) Idaho National Laboratory (INL). The Feedstock Logistics Design Case for Multiple Conversion Pathways. Idaho National Laboratory, Idaho Falls, ID, **2014**; https://bioenergy.inl.gov/Reports/Feedstock%20Supply%20System%20Design%20and%20Analysis.pdf (accessed January 22, 2019).

(32) Hess, J. R.; Kenney, K. L. Commodity-Scale Production of an Infrastructure-Compatible Bulk Solid from Herbaceous Lignocellulosic Biomass. Idaho National Laboratory, Idaho Falls, ID, **2009**, https://bioenergy.inl.gov/Reports/Uniform%20Format%20Bioenergy%20Feedstock.pdf

(accessed January 22, 2019).
(33) U.S. Department of Agriculture. Usual Planting and Harvesting Dates for U.S. Field Crops. U.S. Department of Agriculture, *Washington, DC*, **2010**; http://usda.mannlib.cornell.edu/usda/nass/planting//2010s/2010/planting-10-29-2010.pdf (accessed June 28, 2018)
(34) Borreani, G.; Tabacco, E.; Schmidt, R. J.; Holmes, B. J.; Muck, R. E. Silage review: Factors affecting dry matter and quality losses in silages. *J. Dairy Sci.* **2018**, *101* (5), 3952–3979, DOI 10.3168/jds.2017-13837.
(35) Humbird, D.; Davis, R.; Tao, L.; Kinchin, C.; Hsu, D.; Aden, A.; Schoen, P.; Lukas, J.; Olthof, B.; Worley, M. *Process design and economics for biochemical conversion of lignocellulosic biomass to ethanol: dilute-acid pretreatment and enzymatic hydrolysis of corn stover*; National Renewable Energy Laboratory (NREL), Golden, CO., **2011**; https://www.nrel.gov/docs/fy11osti/47764.pdf (accessed January 22, 2019).
(36) Aden, A.; Ruth, M.; Ibsen, K.; Jechura, J.; Neeves, K.; Sheehan, J.; Wallace, B.; Montague, L.; Slayton, A.; Lukas, J. *Lignocellulosic biomass to ethanol process design and economics utilizing co-current dilute acid prehydrolysis and enzymatic hydrolysis for corn stover*; National Renewable Energy Lab., Golden, CO.(US), **2002**; https://www.nrel.gov/docs/fy02osti/32438.pdf (accessed January 22, 2019).
(37) Davis, R.; Tao, L.; Tan, E. C. D.; Biddy, M. J.; Beckham, G. T.; Scarlata, C.; Jacobson, J.; Cafferty, K.; Ross, J.; Lukas, J. *Process design and economics for the conversion of lignocellulosic biomass to hydrocarbons: dilute-acid and enzymatic deconstruction of biomass to sugars and biological conversion of sugars to hydrocarbons*; National Renewable Energy Laboratory (NREL), Golden, CO., **2013**; https://www.nrel.gov/docs/fy14osti/60223.pdf (accessed January 22, 2019).
(38) Neupane, B.; Konda, N. M.; Singh, S.; Simmons, B. A.; Scown, C. D. Life-Cycle Greenhouse Gas and Water Intensity of Cellulosic Biofuel Production Using Cholinium Lysinate Ionic Liquid Pretreatment. *ACS Sustain. Chem. Eng.* **2017**, *5* (11), 10176–10185, DOI 10.1021/acssuschemeng.7b02116.
(39) Sun, J.; Shi, J.; Konda, N. M.; Campos, D.; Liu, D.; Nemser, S.; Shamshina, J.; Dutta, T.; Berton, P.; Gurau, G. Efficient dehydration and recovery of ionic liquid after lignocellulosic processing using pervaporation. *Biotechnol. Biofuels* **2017**, *10* (1), 154, DOI 10.1186/s13068-017-0842-9.
(40) Hiremath, A.; Kannabiran, M.; Rangaswamy, V. 1, 3-Propanediol production from crude glycerol from jatropha biodiesel process. *N. Biotechnol.* **2011**, *28* (1), 19–23, DOI 10.1016/j.nbt.2010.06.006.
(41) Chen, X.; Zhang, D.-J.; Qi, W.-T.; Gao, S.-J.; Xiu, Z.-L.; Xu, P. Microbial fed-batch production of 1, 3-propanediol by Klebsiella pneumoniae under micro-aerobic conditions. *Appl. Microbiol. Biotechnol.* **2003**, *63* (2), 143–146, DOI 10.1007/s00253-003-1369-5.
(42) Mendez-Perez, D.; Alonso-Gutierrez, J.; Hu, Q.; Molinas, M.; Baidoo, E. E. K.; Wang, G.; Chan, L. J. G.; Adams, P. D.; Petzold, C. J.; Keasling, J. D.; Lee, T.S. Production of jet fuel precursor monoterpenoids from engineered Escherichia coli. *Biotechnol. Bioeng.* **2017**,114, 1703-1712, DOI 10.1002/bit.26296.
(43) Murray, S. C.; Rooney, W. L.; Mitchell, S. E.; Sharma, A.; Klein, P. E.; Mullet, J. E.;

Kresovich, S. Genetic improvement of sorghum as a biofuel feedstock: II. QTL for stem and leaf structural carbohydrates. *Crop Sci.* **2008**, *48* (6), 2180-2193, DOI 10.2135/cropsci2008.01.0068.

(44) Zhao, Y. L.; Dolat, A.; Steinberger, Y.; Wang, X.; Osman, A.; Xie, G. H. Biomass yield and changes in chemical composition of sweet sorghum cultivars grown for biofuel. *F. Crop. Res.* **2009**, *111* (1), 55–64, DOI 10.1016/j.fcr.2008.10.006.

(45) Li, B.-Z.; Balan, V.; Yuan, Y.-J.; Dale, B. E. Process optimization to convert forage and sweet sorghum bagasse to ethanol based on ammonia fiber expansion (AFEX) pretreatment. *Bioresour. Technol.* **2010**, *101* (4), 1285–1292, DOI 10.1016/j.biortech.2009.09.044.

(46) Wu, L.; Arakane, M.; Ike, M.; Wada, M.; Takai, T.; Gau, M.; Tokuyasu, K. Low temperature alkali pretreatment for improving enzymatic digestibility of sweet sorghum bagasse for ethanol production. *Bioresour. Technol.* **2011**, *102* (7), 4793–4799, DOI 10.1016/j.biortech.2011.01.023.

(47) Corredor, D. Y.; Salazar, J. M.; Hohn, K. L.; Bean, S.; Bean, B.; Wang, D. Evaluation and characterization of forage sorghum as feedstock for fermentable sugar production. *Appl. Biochem. Biotechnol.* **2009**, *158* (1), 164-179, DOI 10.1007/s12010-008-8340-y.

(48) Koradiya, M.; Duggirala, S.; Tipre, D.; Dave, S. Pretreatment optimization of Sorghum pioneer biomass for bioethanol production and its scale-up. *Bioresour. Technol.* **2016**, *199*, 142–147, DOI 10.1016/j.biortech.2015.08.156.

(49) Qureshi, N.; Liu, S.; Hughes, S.; Palmquist, D.; Dien, B.; Saha, B. Cellulosic Butanol (ABE) Biofuel Production from Sweet Sorghum Bagasse (SSB): Impact of Hot Water Pretreatment and Solid Loadings on Fermentation Employing Clostridium beijerinckii P260. *BioEnergy Res.* **2016**, *9* (4), 1167–1179, DOI 10.1007/s12155-016-9761-z.

(50) Meyer, H.; Minas, W.; Schmidhalter, D. In Industrial Biotechnology Products and Processes Edited by Christoph Wittmann and James C. Liao. Wiley-VCH Verlag GmbH & Co.KGaA, Boschstr. 12, 69469 Weinheim, Germany.**2017**, pp1–53.

(51) Hannon, J.; Bakker, A.; Lynd, L.; Wyman, C. Comparing the scale-up of anaerobic and aerobic processes. In *Annual Meeting of the American Institute of Chemical Engineers: Salt Lake City*; 2007; http://www.bakker.org/cfm/publications/AIChE-2007-Hannon.pdf (accessed March 07, 2018).

(52) Fernández-Sandoval, M. T.; Galíndez-Mayer, J.; Moss-Acosta, C. L.; Gosset, G.; Martinez, A. Volumetric oxygen transfer coefficient as a means of improving volumetric ethanol productivity and a criterion for scaling up ethanol production with Escherichia coli. *J. Chem. Technol. Biotechnol.* **2017**, *92* (5), 981–989, DOI 10.1002/jctb.5087.

(53) Huang, Y.; Li, Z.; Shimizu, K.; Ye, Q. Co-production of 3-hydroxypropionic acid and 1, 3-propanediol by Klebseilla pneumoniae expressing aldH under microaerobic conditions. *Bioresour. Technol.* **2013**, *128*, 505–512, DOI 10.1016/j.biortech.2012.10.143.

(54) Kang, A.; Meadows, C. W.; Canu, N.; Keasling, J. D.; Lee, T. S. High-throughput enzyme screening platform for the IPP-bypass mevalonate pathway for isopentenol production. *Metab. Eng.* **2017**, *41*, 125–134, DOI 10.1016/j.ymben.2017.03.010.

(55) Brandt-Talbot, A.; Gschwend, F. J. V; Fennell, P. S.; Lammens, T. M.; Tan, B.; Weale, J.; Hallett, J. P. An economically viable ionic liquid for the fractionation of lignocellulosic biomass. *Green Chem.* **2017**,19, 3078-3102, DOI 10.1039/C7GC00705A.

(56) Argon National Laboratory (ANL). GREET® Model; Argon National Laboratory: Lemont, IL, **2016**; https://greet.es.anl.gov/ (accessed March 07, 2017).
(57) Ecoinvent. Ecoinvent - The World's most consistent & transparent Life Cycle Inventory database. **2017**, https://www.ecoinvent.org/ (accessed June 18, 2018).
(58) National Renewable Energy Laboratory (NREL). U.S. Life Cycle Inventory Database; National Renewable Energy Laboratory (NREL): Golden, CO, 2011; http://www.nrel.gov/lci/ (accessed March 25, 2017).
(59) Scown, C. D.; Horvath, A.; McKone, T. E. Water footprint of US transportation fuels. *Environ. Sci. Technol.* **2011**, *45* (7), 2541–2553, DOI 10.1021/es102633h.
(60) EIA, Gasoline and Diesel Fuel Update, US Energy Information Administration, Washington, DC, 2018; https://www.eia.gov/petroleum/gasdiesel/ (accessed January 22, 2019).
(61) Scown, C. D.; Gokhale, A. A.; Willems, P. A.; Horvath, A.; McKone, T. E. Role of lignin in reducing life-cycle carbon emissions, water use, and cost for United States cellulosic biofuels. *Environ. Sci. Technol.* **2014**, *48* (15), 8446–8455, DOI 10.1021/es5012753.
(62) Baral, N.R.; Sundstrom, E.R.; Das, L.; Gladden, J.; Eudes, A.; Mortimer, J.C.; Mukhopadhyay, A.; Scown, C. D. Approaches for More Efficient Biological Conversion of Lignocellulosic Feedstocks to Biofuels and Bioproducts. *ACS Sustain. Chem. Eng.* **2019**, 7(10), 9062-9079, DOI 10.1021/acssuschemeng.9b01229.
(63) Climate Policy Initiative. California Carbon Dashboard. California, USA, **2018**; https://climatepolicyinitiative.org/publication/california-carbon-dashboard/ (accessed January 22, 2019).
(64) U.S. EPA. The Social Cost of Carbon. United States Environmental Protection Agency, Washington, DC, USA, **2017**; https://19january2017snapshot.epa.gov/climatechange/social-cost-carbon.html (accessed April 24, 2019).
(65) Ricke, K.; Drouet, L.; Caldeira, K.; Tavoni, M. Country-level social cost of carbon. *Nature Climate Change.* 2018, 8(10), 895-900, DOI 10.1038/s41558-018-0282-y.